Ninth International Conference on Computational Fluid Dynamics (ICCFD9), Istanbul, Turkey, July 11-15, 2016

ICCFD9-2016-123

Considerations of Stress Limiter for the SST Turbulence Model in Dual Throat Nozzle Predictions

R. Tharwat[1] M. El-Samanoudy[1] and A. M. R. El-Baz[2]

[1]Mechanical Power Engineering Department, Ain Shams University, Cairo 11517, Egypt
[2]Mechanical Engineering Department, The British University in Egypt, El Sherouk City, Cairo, Egypt

Corresponding author: Ahmed El Baz, email: ahmed.elbaz@bue.edu.eg, Tel +20 100 164 33 91

Abstract: The k-ω Shear Stress Transport (SST) Turbulence model introduced by Menter has been widely used successfully as one of the two-equation eddy viscosity models. In this paper the Menter k-ω SST turbulence model is used and calibrated to simulate the Dual Throat Nozzle (DTN) for fluidic thrust vectoring techniques. Despite the SST model advantages, in the DTN case the model shows over-prediction for the separated flow in recess cavity zone of DTN due to the effects of adverse pressure gradient on the boundary layer. Moreover, the model prediction for separated flow shows sensitivity to the nozzle geometry. To improve the Menter SST Model results for DTN application to coincide with the experimental data and to avoid the over-prediction for the separated flow, the present study implements the shear stress limiter element in the Menter SST Model by modifying the eddy viscosity term via adjusting a structure parameter (a_1). The structure parameter is used to prevent the calculated turbulent shear stress from exceeding preserved fraction of turbulent kinetic energy. Also adjustments to the DTN geometry is proposed to decrease the flow separation inside the recess cavity. Preliminary results of adjusting the structure parameter a_1 value near 0.34 accompanied by geometrical refinements of throat edge shows improvement in the SST model results to be consistent with the experimental results of NASA Langley research center jet exit test facility.

Keywords: Shear Stress Transport Model, k-omega Turbulence Model, Dual Throat Nozzle, Fluidic Thrust Vectoring, Aeronautics.

Nomenclature:

a_1	structure parameter	ε	turbulent dissipation rate
Ae	Nozzle exit area	μ_t	dynamic eddy viscosity
At	Nozzle throat area	μ	dynamic viscosity
C_{Lim}	shear stress limiting coefficient	κ	von Karman constant
D	distance from wall	τ_{ij}^T	turbulent stress tensor
hn	nozzle inlet height	ω	specific turbulent dissipation rate = ε/k
ht	upstream throat height		
k	turbulent kinetic energy	Ω	vorticity
L	Cavity length		
P_k	production of turbulent kinetic energy		
S_{ij}	mean rate of strain tensor		

1 Introduction

The development of CFD turbulence models is highly needed to improve the prediction accuracy of aeronautical complex turbulent flows with strong adverse pressure gradients and separation interaction with boundary layer flow. The Reynolds average Navier Stokes (RANS) approach is the reasonable widely used computational method due to its reliability and high accuracy low cost computational fluid dynamic (CFD) method. A recent CFD workshop [1] which focused on the calculations of a set of Shock wave boundary layer interaction (SWTBLI) cases was organized by the American Institute of Aeronautics and Astronautics (AIAA), using Reynolds-averaged Navier-Stokes (RANS) solvers and Large-Eddy Simulations (LES) models. The workshop resulted that RANS methods have difficulties to predict the details of the SWTBLI problems. Therefore, further developments of turbulence models are needed to improve CFD results in comparison with experimental data.

Menter's k-ω Shear Stress Transport (SST) Turbulence model [2] has shown relatively accurate results for a range of small separation behavior of mild adverse pressure gradients in subsonic flows. The model has been designed for predicting the adverse pressure gradient flows where most of the two-equation models have difficulties to predict successfully. In application case of the Dual Throat Nozzle (DTN) [3, 4] concept for fluidic thrust vectoring techniques, which was originally developed by NASA Langley Research Center (LaRC) to achieve higher capabilities to the thrust vectoring efficiencies, separation region occurs in the DTN recess cavity, and Menter's k-ω SST model showed over-prediction of the flow separations size. While the formulation of baseline k-ω turbulence model (BSL) was introduced by Menter [6], without the stress limiter, which tends to under-predict the size of shock-induced separations.

Dual Throat Nozzle concept has proved good thrust vectoring capabilities [3,4]. The nozzle geometry is shown in Fig. 1. Several geometric parameters affect nozzle vectoring performance such as cavity length, divergence angle of the recess cavity and convergence angle of exit nozzle. A comprehensive set of tests have been carried out by LaRC group [5,6]. The nozzle geometry considered in the present study represent the optimum geometry recommended for DTN which achieves the best vectoring efficiency. In non-vectored mode the DTN is considered as supper sonic converging-diverging-converging nozzle with two minimum throats, Fig. 1, with expansion ratio A_e/A_t=1 and NPR of 4.0. The main geometrical design parameters defining the nozzle are listed in Table 1. The throat shape is considered to be sharp edged. However, curved edge shape with different values of the radius R_1 were also investigated.

2 Methods

Computational domain and boundary conditions

The adopted computational domain and boundary conditions are also presented in Fig. 1. The atmospheric zone following DTN is represented with length L_{F1} of 120 [mm] (L_{F1}/h_e=4) and height L_{F2} of 240 [mm] (L_{F2}/h_e=8) [20]. The exit far downstream boundary and the entrainment plane normal to nozzle exit were considered to be constant pressure boundaries while the lateral sides were considered to be wall boundary. The ambient conditions for the simulation were set at 101325 [Pa] and 290 [°K]. The main inlet of the nozzle was specified as a pressure inlet with total nozzle pressure ratio NPR = 4.0. The walls of the nozzle were set as adiabatic no-slip wall boundary condition.

Numerical Mesh

Mesh generation for the nozzle computational domain was optimized and controlled by dividing the domain mesh into segments, which gives an availability to optimize and generate the required mesh

quality for each flow region with minimum computational recourses. The different mesh zones are shown in Fig. 2. The nozzle internal domain was divided to three meshing segments, the near wall segment with fine element size for the near wall flow region, the inner core segment with coarser element size for the nozzle core flow region, and the transition meshing segment to perform smooth transformation of element size between the previous two segments. Near wall function Y^+ of value less than unity ($Y^+ <1$) was ensured for the k-ω model, while Y+ value between 30 and 300 ($30 < Y+ <300$) was considered to k-ε model. A mesh independency test was performed which indicated the high sensitivity of the predicted results to the mesh element size and the near wall function Y^+ in the near wall region and less sensitivity to the element size in the nozzle inner core free stream region.

Table 1. Dual Throat Nozzle (DTN) design parameters [4]

Parameter	Value
Cavity Length (L)	76.2 [mm]
Divergence Angle (θ_1)	10 [Degree]
Downstream Convergence Angle (θ_2)	20 [Degree]
Upstream Throat Height (h_t)	29.2 [mm]
Downstream Throat Height (h_e)	29.2 [mm]
Upstream convergence Angle (θ_p)	30 [Degree]
Nozzle inlet height (h_n)	80 [mm]
Exterior region : Normal to axis Far Filled (L_{F2})	120 [mm]
Exterior region : Parallel to axis Far Filled (L_{F2})	240 [mm]

Baseline (BSL) k-ω model (k-ω BSL)

The k-ω Baseline (BSL) model introduced by Menter [5] is similar to the original k-ω model of Wilcox [18], without its strong dependency on arbitrary freestream values. The BSL model is identical to the Wilcox model in the boundary-layer region but changes gradually to the standard k–ε model in the free stream inner region. The BSL model is preliminary version of the Shear-Stress Transport (SST) model. The results of the BSL model are comparable to those of the original k-ω model, without the undesirable free stream dependency.

Menter SST k - ω Model (k-ω SST)

The k-ω Shear Stress Transport turbulent model was introduced by Menter in 1994 [2] to improve the prediction of the adverse pressure gradient cases and to deal with the problems due to the strong sensitivity of original k-ω to the free stream flow. The model is two-equation eddy viscosity model, widely used in CFD to model the compressible and incompressible turbulent flows. The SST model is expressed in k-ω formulation and combines two of the most widely used models k-ω and k-ε turbulence models. The SST model uses the k-ω model formulation in the inner region of the boundary viscous sublayer and switches to the k-ε model formulation in the free-stream region, The SST model has greatly benefited from the advantages of several desirable elements in the two models and eliminates the common problems of the k-w models free stream strong sensitivity, and the problems of the k-ε in the near wall viscous layer. This merging makes the SST model more precise for a larger variety of the flows than the standard models.

The SST model is merit for its good behavior in the adverse pressure gradients and separated flows. However, as per the work of Tan [15] and Oliver et al [16] the model produces a bit too large

turbulence levels in the large normal strain regions, as the stagnation regions and the strong acceleration regions and to over-predict separation cases more than the standard k-ε model.
The model equations can be written using Favre averaged velocity field [2]

The k-equation:

$$\frac{\partial(\rho k)}{\partial t}+\frac{\partial(\rho U_j k)}{\partial x_j}=P_k-\beta^*\rho\omega k+\frac{\partial}{\partial x_j}\left((\mu+\sigma_k\mu_t)\frac{\partial k}{\partial x_j}\right) \tag{1}$$

The ω-equation:

$$\frac{\partial(\rho\omega)}{\partial t}+\frac{\partial(\rho U_j\omega)}{\partial x_j}=\frac{\gamma}{\nu_t}P_k-\beta\rho\omega^2+\frac{\partial}{\partial x_j}\left((\mu+\sigma_\omega\mu_t)\frac{\partial\omega}{\partial x_j}\right)+2(1-F_1)\rho\sigma_{\omega2}\frac{1}{\omega}\frac{\partial k}{\partial x_j}\frac{\partial\omega}{\partial x_j} \tag{2}$$

where:

$$P_k=\tau_{ij}^T\frac{\partial u_i}{\partial x_j} \tag{3}$$

$$\tau_{ij}^T=\mu\left(2S_{ij}-\frac{2}{3}\frac{\partial u_k}{\partial x_k}\delta_{ij}\right)-\frac{2}{3}\rho k\delta_{ij} \tag{4}$$

$$S_{ij}=\frac{1}{2}\left(\frac{\partial u_j}{\partial x_i}+\frac{\partial u_i}{\partial x_j}\right) \tag{5}$$

$$F_1=\tanh[(\arg_1)^4] \tag{6}$$

$$\arg_1=\min\left(\max\left(\frac{\sqrt{k}}{\beta^*\omega d};\frac{500\nu}{\omega d^2}\right);\frac{4\rho\sigma_{\omega2}k}{CD_{k\omega}d^2}\right) \tag{7}$$

$$CD_{k\omega}=\max\left(2\rho\sigma_{\omega2}\frac{1}{\omega}\frac{\partial \mathrm{k}}{\partial x_j}\frac{\partial \omega}{\partial x_j};1.0\times10^{-20}\right) \tag{8}$$

The turbulent viscosity is defined by:

$$\mu_t=\frac{\rho a_1 k}{\max(a_1\omega;\Omega F_2)}=\frac{\rho k}{\max(\omega;\Omega F_2/a_1)} \tag{9}$$

where

$$F_2=\tanh[(\arg_2)^2] \tag{10}$$

$$\arg_2=\max\left(2\frac{\sqrt{k}}{\beta^*\omega d};\frac{500\nu}{\omega d^2}\right) \tag{11}$$

The constants (set 1) for the inner mode of the boundary layer are :

$$\gamma_1=\frac{\beta_1}{\beta^*}-\frac{\sigma_{\omega1}\kappa^2}{\sqrt{\beta^*}},\qquad \sigma_{k1}=0.85\,,\qquad \sigma_{\omega1}=0.5\,,\qquad \beta_1=0.075\,,$$

The constants (ϕ_2) for the transformed *k*-ε model (set 2) are :

$$\gamma_2=\frac{\beta_2}{\beta^*}-\frac{\sigma_{\omega2}\kappa^2}{\sqrt{\beta^*}},\qquad \sigma_{k2}=1.00\,,\qquad \sigma_{\omega2}=0.856\,,\qquad \beta_2=0.0828,$$

These constants are blended using the same switching function, F_1 found in the model equations such that $\emptyset=F_1\emptyset_1+(1-F_1)\emptyset_2$ for any of the given parameters.

The constant values as follows:

$$a_1=0.31\,,\qquad \kappa=0.41\,,\qquad \beta^*=0.09\,,$$

Shear Stress Limiter

Menter [2] developed k-ω SST model, where the turbulent shear stress in a boundary layer is proportional to the turbulent kinetic energy through a constant

$$\tau = -\rho\overline{u'v'} = \rho a_1 k \tag{12}$$

The proportionality constant, a_1, is commonly referred as the structured parameter and used as the limiter for the original Menter k-ω SST model, which calculates the turbulent shear stress from Equation.(4) and the form of vorticity magnitude (Ω), Equation.(9), to limit the eddy viscosity to the minimum of ρk/ω and $\rho a_1 k/\Omega F_2$, where according to Menter [8] the SST model employs the F_2 function value to unity in the inner three-fourths of a zero-pressure gradient boundary layer and drops to zero outside boundary layers, enabling the shear stress limiter to be turned off outside boundary layers, which is an advantage of the hybrid model formulation.

The Default value for the SST model of a_1=0.31 set by Menter [2] shows success for the attached boundary layers or mild adverse pressure gradient flows leading to relatively small separations. Coakley [9] developed a *q-ω* model which also used a shear stress limiter with a value for this constant of 0.30. Bradshaw et al [10] developed a one-equation model based on the same relation of the turbulent shear stress to the turbulent kinetic energy using another structure parameter term with a value of 0.30. Rose [11] investigated the value of a_1 for a homogenous free shear layer flow and found a_1 to be approximately 0.35. Edwards et al. [12] concluded that a_1 = 0.356 according to agreement with experimental results for a Mach 5 compression corner problem as known case for (SWTBLI) flows. Nicholas et al [17] investigation utilized a value for a_1 closer to 0.355 improved the separation flow prediction. Other reported efforts have investigated a different value than a_1 = 0.31 for shock-boundary layer dominated flows.

In the Wilcox's k-ω model [18], the eddy viscosity term is written:

$$\mu_t = \rho\nu_t = \frac{\rho a_1 k}{max(a_1\omega, C_{lim}\, S\, F_2\ )} \tag{13}$$

where a_1 =0.31 , $S = \sqrt{2S_{ij}S_{ij}}$ and F_2 is second blending function is written:

$$F_2 = tanh\left[\left[max\left(\frac{2\sqrt{k}}{\beta^*\omega d}, \frac{500\nu}{d^2\omega}\right)\right]^2\right] \tag{14}$$

where d is distance to the nearest wall and ν is the kinematic viscosity.

The value of C_{lim}=0 can be corresponding to the Menter's baseline model (BSL) and the value of C_{lim}=1.0 is corresponding to the Menter's Shear stress transport model (SST). According to investigated by Tan and Jin [15] the experimental results for SWTBLI cases the C_{lim}=0 under-predicts the separation region, while using C_{lim} =1.0 over-predicts the separation region.

Wilcox in his most recent model implements a shear stress limiter C_{lim} to the eddy viscosity term as per Equation.(13). Wilcox uses the rate-of-strain tensor instead of vorticity and the coefficient C_{lim} rather than a_1. In Wilcox model the stress limiter is applied inside and outside the boundary layer,

while the Menter SST model the F_2 function applies the shear stress limiter inside the boundary layer only. The structure parameter can be related to C_{lim} by

$$a_1 = \frac{1}{C_{lim}}\sqrt{\beta^*} \tag{15}$$

By using Wilcox's model coefficients the value of structure parameter is calculated to be $a_1 = 0.342$, and by using the vorticity magnitude Ω the effective structure parameter is set to be $a_1 = 0.316$. This difference in the Stress limiter implementation in the Wilcox's and Menter's Models was investigated by Tan and Jin [15] with different values of a_1, and expressed through the context of the C_{lim} parameter.

3 Results

The RANS equations were solved using the ANSYS-FLUENT. An initial run using the original Menter k-ω SST Model [2] and k-ε model [7] was performed to the DTN geometry, to determine the performance of both models to predict flow behaviour inside DTN. Figure 3 shows the predicted static pressure distribution on the nozzle upper surface wall and the nozzle centerline using k-ε model. Figure 4 similar results obtained using k-ω SST model. Both figures also show the experimental results for pressure distribution on the nozzle upper surface [4]. The centerline static pressure results show that the nozzle flow behavior is subsonic flow. However, the pressure distribution on the upper surface shows lower throat pressure than the centerline due to two dimensional effects. Since the NPR is 4, the exit pressure ratio is very close to 0.25. The flow expands outside the nozzle to the ambient pressure. The cavity allows the nozzle internal flow to expand inside the nozzle as in a conventional

convergent-divergent nozzle before encountering the second convergent ramp prior to the nozzle exit, thus shifting the design nozzle pressure ratio slightly higher for this nozzle [4]. The k-ε model results on the upper surface, Fig. 3, show good agreement with the experimental data in the pressure recovery zone of the nozzle cavity. However, the k-ω SST model results, Fig. 4, do not show the measured pressure recovery.

Figures 5 and 6 show the predicted Mach number contours for the DTN at NPR = 4.0 using k- ε model and k-ω SST model, respectively. The predicted Mach number contours clearly show that the flow expands outside the DTN to reach Mach numbers of 1.8. The predicted Mach contours results for k-ω SST model, Fig. 6, show flow separation along upper and lower walls of the nozzle cavity. This is similar to shadowgraph results reported in [4]. The k- ε model results show weaker separation. The near wall flow behaviour of both models is further explained in enlarged view of the nozzle upstream throat, Fig. 7 and Fig. 8. The flow near nozzle edge forms localized supersonic regions due to area change where Mach number values higher than 1 exist. Ine strong separated flow predicted by the k-ω SST model is very clear in Fig. 8 and a weak shock wave is formed near the separation point.

Effect of the nozzle throat curvature

The concept of curved edge for the upstream throat minimum area is implemented to replace the sharp edge. Two values of the radius R_1 were investigated, R_1=5 and 10 mm, while maintaining the same nozzle throat height h_1=29.2 [mm]. Figure 9 shows the predicted static pressure distribution on the upper nozzle wall for the different cases using k-ω SST model. The results show that using R_1=10 mm results in better agreement with the experimental pressure recovery behaviour. Fig. 10 shows the corresponding predicted Mach number contours. The flow separation is less pronounced compared with sharp edge predictions, Fig. 6. The enlarged view of the separation region is shown in Fig. 11.

The localized supersonic flow region still exists near the nozzle throat and a weak shock wave is also observed.

Effect of the stress limiter

The weak pressure recovery observed in the SST model results is associated with strong flow separation following the upstream throat. The pressure cannot be recovered unless flow tempts to reattach to the upper wall following the nozzle throat. Thus, increasing the shear stress would result in faster pressure recovery. This can be achieved by controlling the stress parameter a_1. Fig. 12 shows the predicted static pressure variation on the upper nozzle surface using different values of the stress limiting structural parameter a_1 and nozzle curved edge with R_1=10 mm. The adjusting of the eddy viscosity structured parameter a_1, improves the results of the Menter k-ω (SST) model to reach an adequate agreement with the experimental results. The pressure recovery behaviour is in close agreement with the experimental measurements for a_1=0.34. Fig. 13 shows the predicted Mach number contours for the this value of a_1. The small increase of the stress coefficient can be seen to cause flow to become closer to the upper surface which lead to higher pressure recovery in the nozzle cavity.
The enlarged view of the predicted Mach number contours near the nozzle edge is shown in Fig. 14. The figure shows that the separated flow is closer to the upper surface as depicted above. There is also a small region where flow accelerates to supersonic state near the edge. A weak shock wave also is observed following Mach number increase. The formation of this shock wave leads to faster pressure recovery downstream.

4 Conclusions

This paper presented flow behaviour predicted by two turbulence models in the DTN case without secondary fluid injection at NPR=4. Examination of SST model results showed that the model produces over-predicted separation behaviour in the divergent part of the nozzle cavity. The standard k-ε model shows better pressure recovery pattern as it predicted weak flow separation. The results also showed that the SST model is sensitive to nozzle edge curvature and better pressure recovery can be obtained if the nozzle edge has a curvature of radius 10 mm. Further, the effect of modifying the stress structure parameter a_1 was investigated. Comparison with experimental data showed that a value of a1= 0.34 yields improved prediction which are consistent with the experimental results.

References

[1] Benek, J., Overview of the 2010 AIAA Shock Boundary Layer Interaction Workshop, AIAA Paper 2010-4821, January 2010.

[2] Menter, F. R., Two Equation Eddy-Viscosity Turbulence Models for Engineering Applications," AIAA Journal, Vol. 32, No. 8, 1994, pp. 1598-1605.

[3] Deere, K. A.; Berrier, B. L.; Flamm, J. D.; and Johnson, S. K.: A Computational Study of a Dual Throat Fluidic Thrust Vectoring Nozzle Concept. AIAA-2003-3502, June 2005.

[4] Flamm, J. D., Deere, K. A ;.; Berrier, B. L.; Johnson, S. K. and Mason, M. L., An Experimental Study of a Dual Throat Fluidic Thrust Vectoring Nozzle Concept. AIAA-2005-3503, July 2005.

[5] Sellam, M. Zmijanovic, V. Leger, L. Chpoun, A., Assessment of gas thermodynamic characteristics on fluidic thrust vectoring performance, International Journal of Heat and Fluid Flow, Volume 53, Pages 156–166, June 2015.

[6] Menter, F.R., “Zonal Two-Equation k-ω Turbulence Models for Aerodynamic Flows,” AIAA Paper 93-2906, July 1993.

[7] B. E. Launder and D. B. Spalding. Lectures in Mathematical Models of Turbulence. Academic Press, London, England. 1972.

[8] Menter, F.R. Review of the shear-stress transport turbulence model experience from an industrial perspective, Int. J. of Computational Fluid Dynamics 23 4 pp 305-316 (2009).

[9] Coakley, T. J., Turbulence Modeling Methods for the Compressible Navier-Stokes Equations," AIAA Paper 83-1693, July 1983.

[10] Bradshaw, P., Ferriss, D. H., and Atwell, N. P., Calculation of Boundary-Layer Development Using the Turbulent Energy Equation, "Journal of Fluid Mechanics, Vol. 28, No. 3, 1967, pp. 593-616.

[11] Rose, W. G., Results of an Attempt to Generate a Homogenous Shear Flow," Journal of Fluid Mechanics, Vol. 25, No. 1, 1966, pp. 97-120.

[12] Edwards, J. R., Choi, J. I., and Boles, J. A., Large-Eddy Reynolds-Averaged Navier-Stokes Simulation of a Mach 5 Compression-Corner Interaction," AIAA Journal, Vol. 46, No. 4, 2008

[13] Kline, S.J., Cantwell, B.J. and Lilley, G.M. proc 1980-81 Stanford Conference on Complex Turbulent Flows, 1981, Stanford University, Stanford, California.

[14] Balabel, A. Hegab, A.M. Nasr, M. El-Behery, S. M., Assessment of turbulence modeling for gas flow in two-dimensional convergent–divergent rocket nozzle , Applied Mathematical Modelling Journal Volume 35, Issue 7, Pages 3408–3422, July 2011.

[15] Tan, J. and Jin., Stress Limiter Consideration for k-w Turbulence Models in Shock Wave/Turbulent Boundary Layer Interactions in Supersonic and Hypersonic Flows ,"AIAA Paper 2011-3980, June 2011.

[16] Oliver, A. B., Lillard, R. P., Schwing A. M., Blasisdell, G. A., and Lyrintzis, A. S., “Assessment of Turbulent Shock Boundary-Layer Interaction Computations Using the overflow Code,” AIAA Paper 2007-104, January 2007

[17] Nicholas J. Georgiadis and Dennis A. Yoder, Recalibration of the Shear Stress Transport Model to Improve Calculation of Shock Separated Flows, AIAA Paper January 7–10, 2013

[18] Wilcox, D. C., Formulation of the k-ω Turbulence Model Revisited," AIAA Journal, Vol. 46, No.11, 2008, pp. 2823-2838.

[19] Wilcox, D. C., Turbulence Modeling for CFD, DCW Industries, 3rd ed., 2006.

[20] Yahaghi, A,. computational study of fluidic thrust vectoring using shock vectoring and separation control , MSAE Thesis , San Jose State University , 2011.

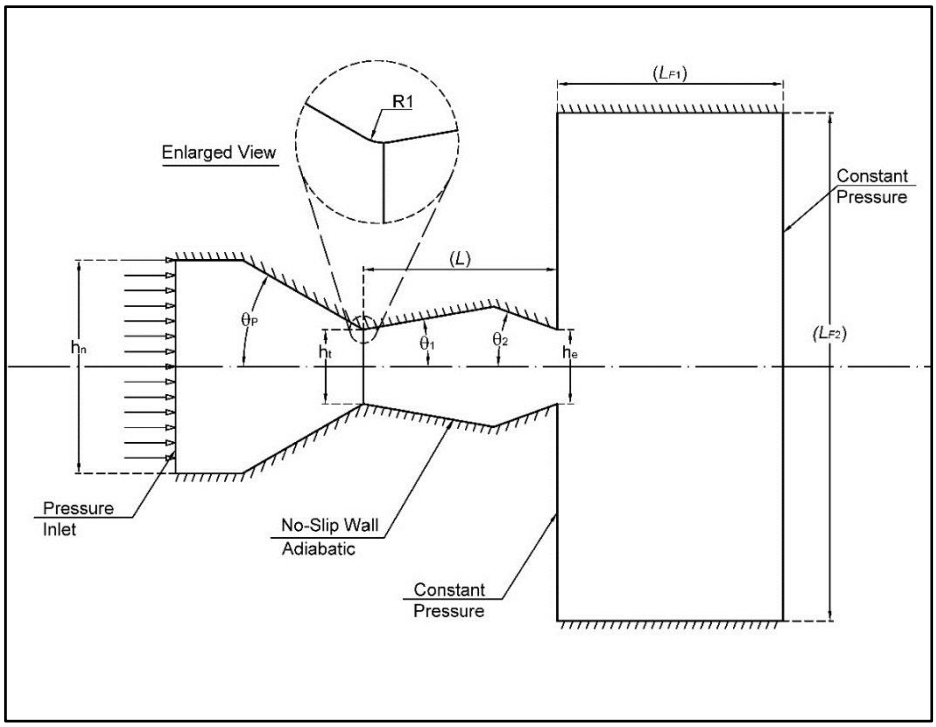

Figure 1. Two dimensional DTN geometry parameters and computational domain.

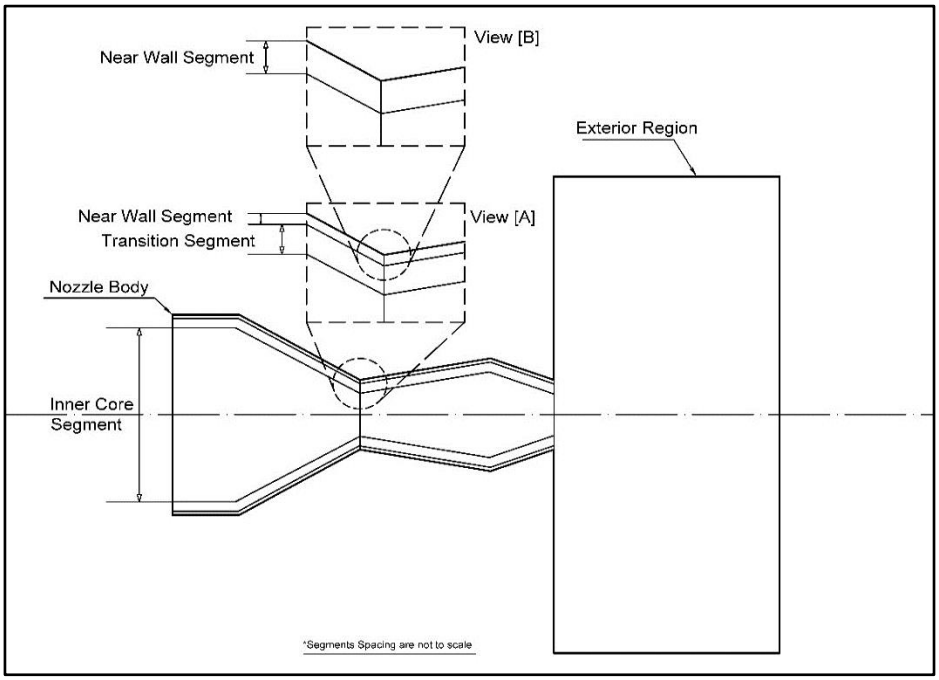

Figure 2. Mesh Segments

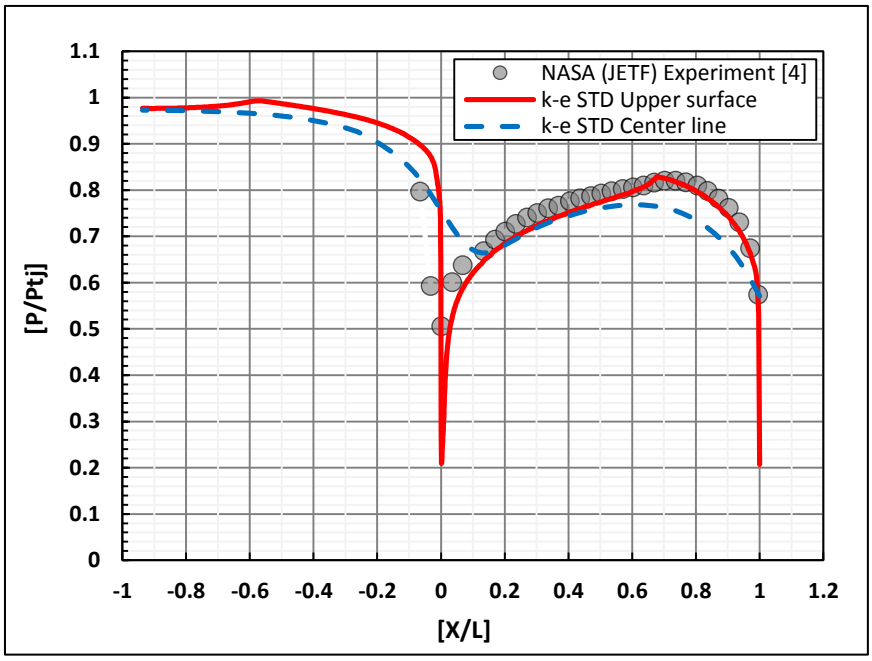

Figure 3. Predicted upper surface and centerline pressure distribution - k-ε model, throat sharp edge, with upper surface pressure experimental measurements.

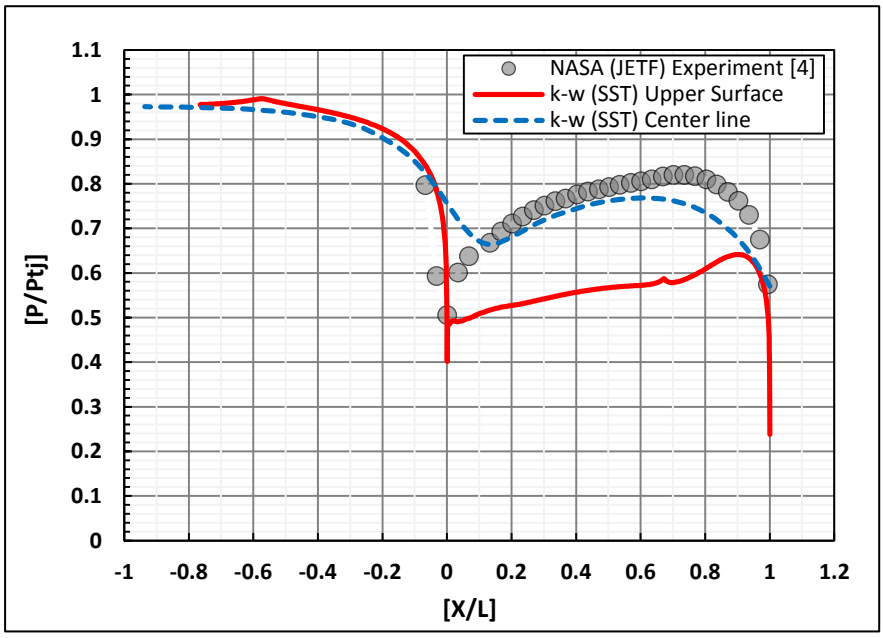

Figure 4. Predicted upper surface and centerline pressure distribution - k-ω SST model, throat sharp edge, with upper surface pressure experimental measurements.

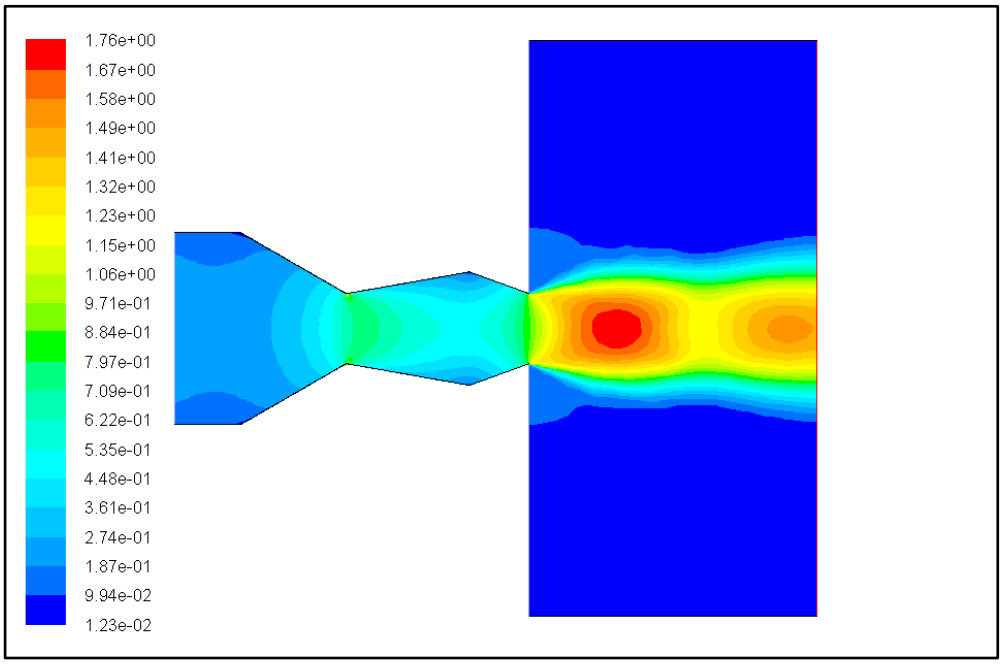

Figure 5. Predicted Mach number contours, k-ε model, NPR=4.0.

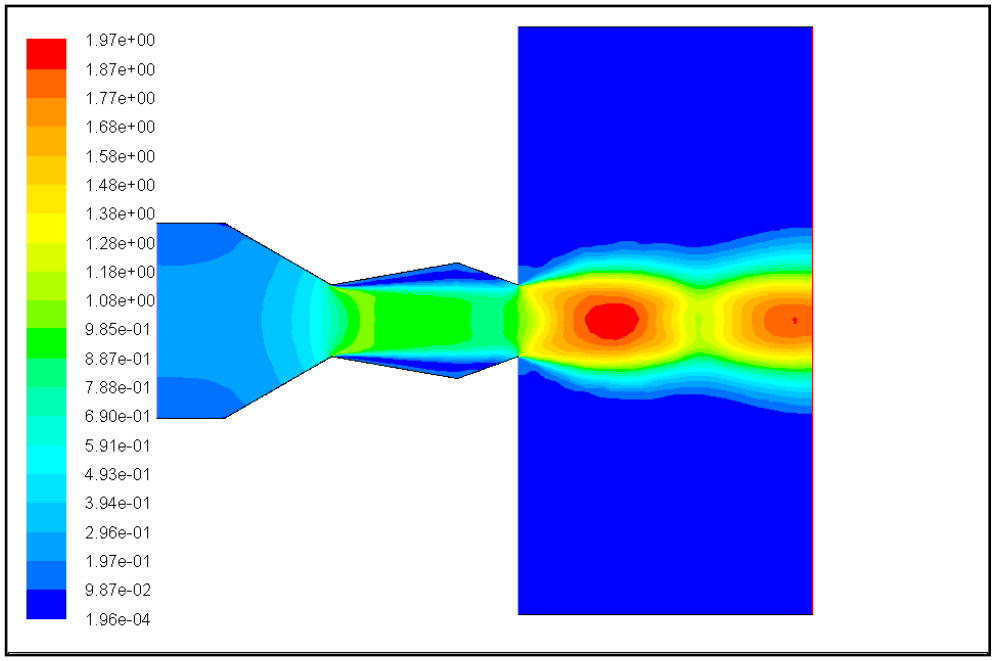

Figure 6. Predicted Mach number contours, k-ω SST model a_1=0.31, NPR = 4.0 .

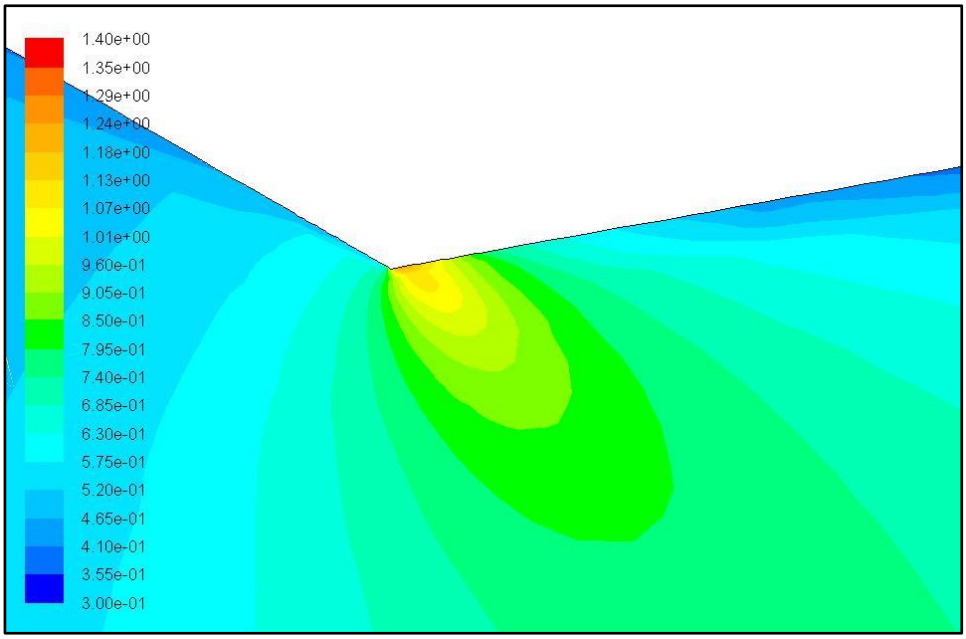

Figure 7 Enlarged throat edge Mach contours, k-ε Model.

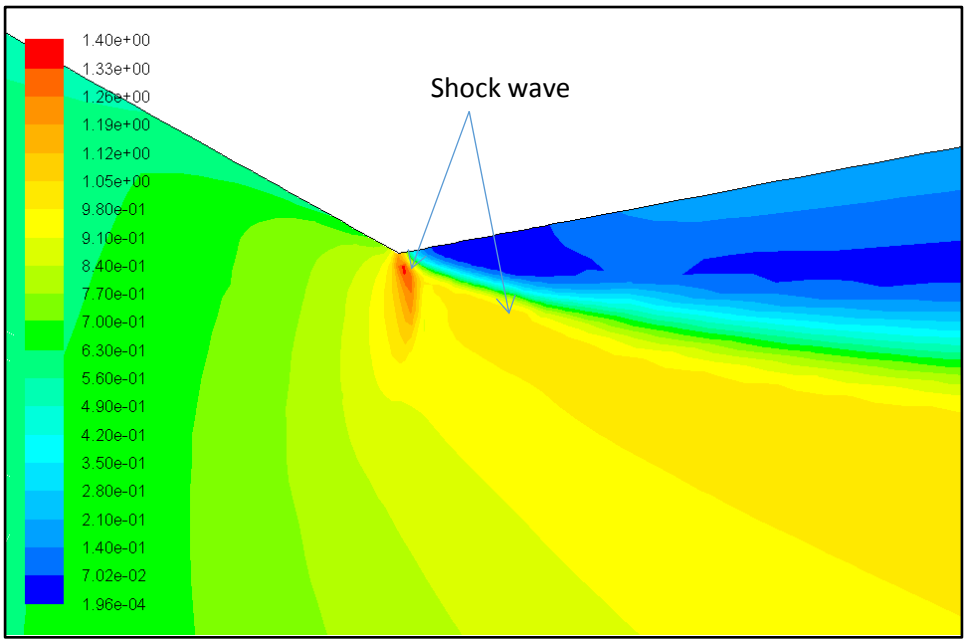

Figure 8. Enlarged throat edge Mach contours, k-ω SST model with structure parameter a_1=0.31.

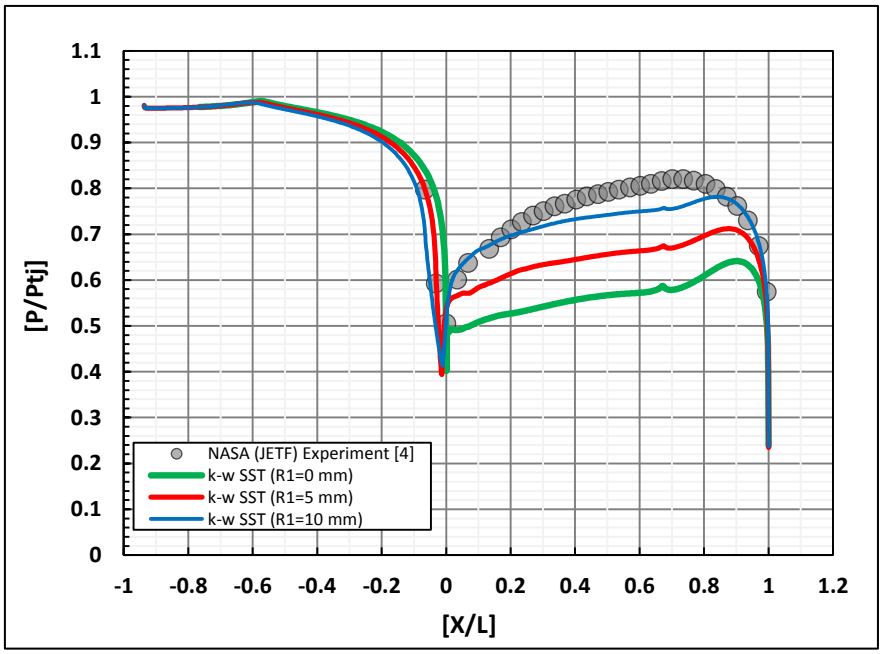

Figure 9 Predicted upper surface pressure distribution for different edge curvature using k-ω SST model with structure parameter a_1=0.31.

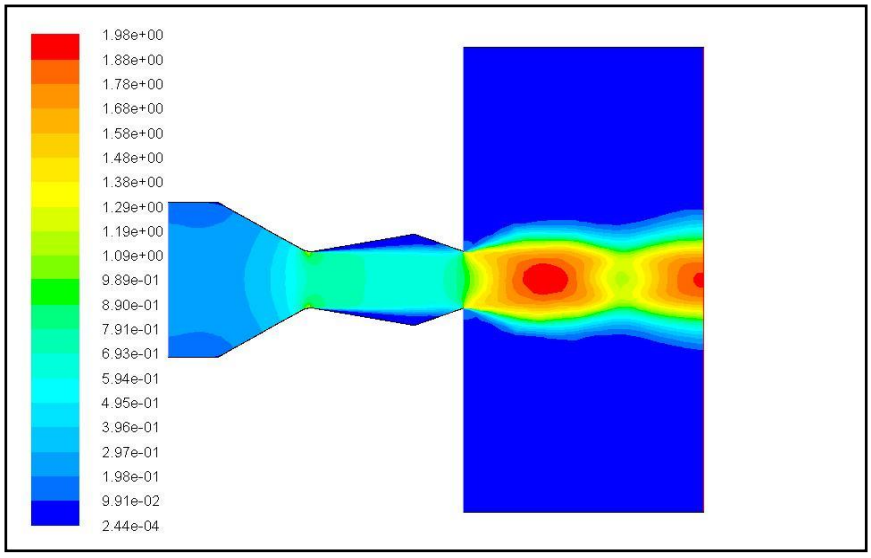

Figure 10 Predicted Mach number contours using k-ω SST model with structure parameter a_1=0.31, R_1=10 mm.

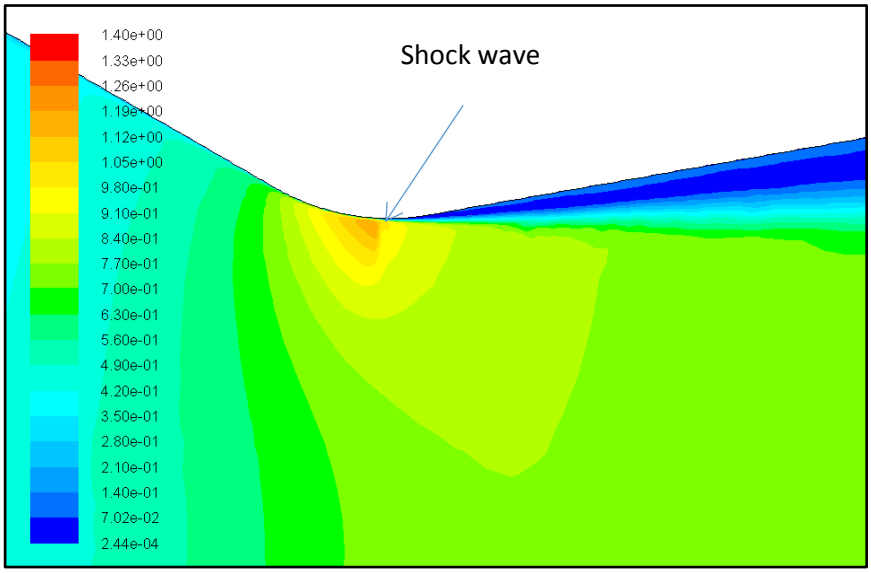

Figure 10. Enlarged throat edge Mach contours, k-ω SST model, throat edge curvature R_1=10 [mm], Structure parameter a_1=0.31 .

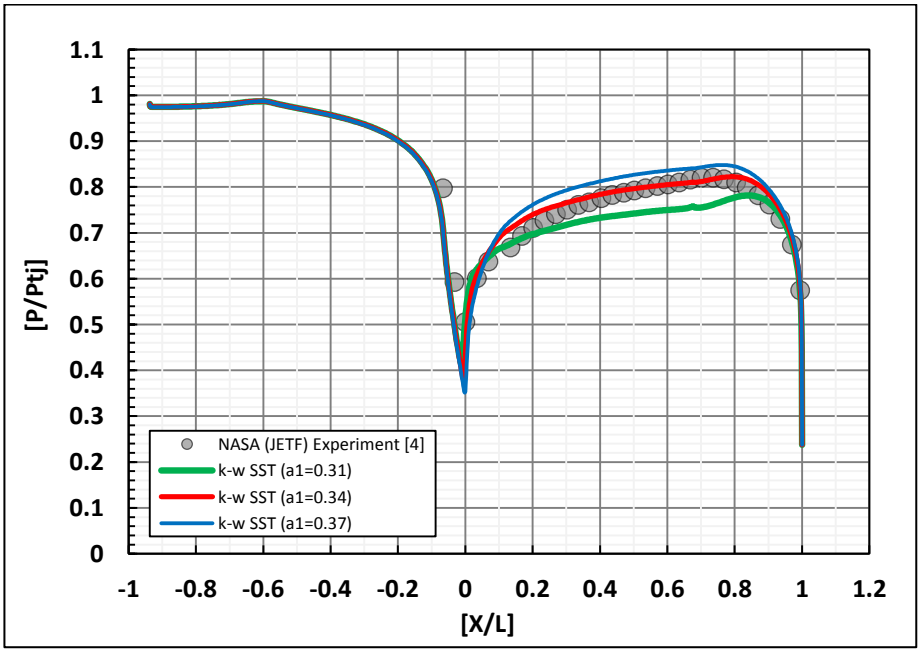

Figure 11 Predicted upper surface pressure distribution using k-ω SST model with different values of structure parameter a_1.

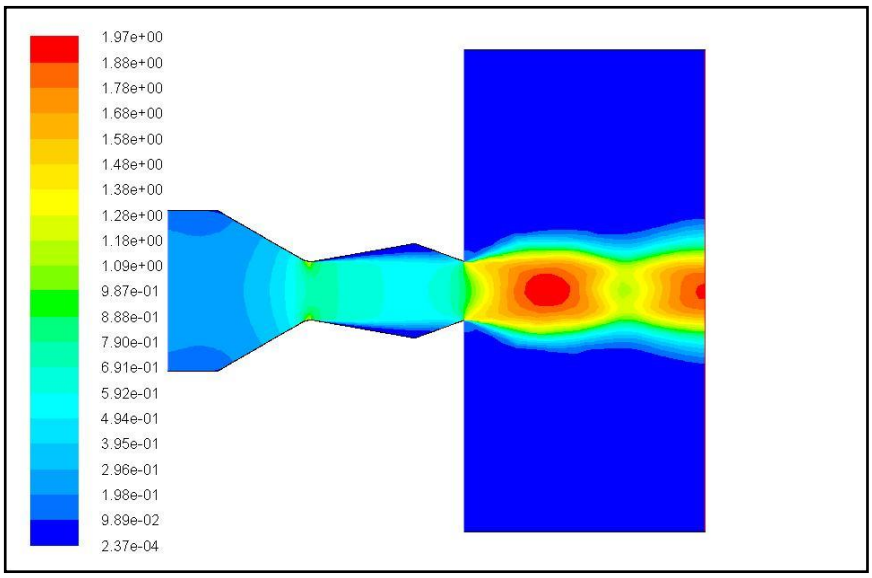

Figure 13 Predicted Mach number contours using k-ω SST model, R_1 = 10 mm, with Structure parameter a_1=0.34

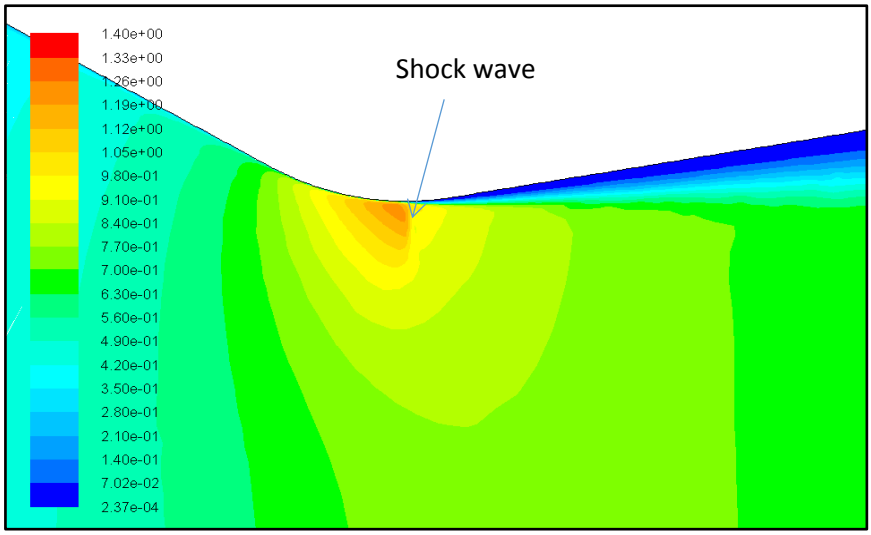

Figure 14 Enlarged throat edge Mach contours, k-ω SST model, R_1=10 [mm], with structure parameter a_1=0.34 .